Received: 8 November 2023 | Revised: 18 March 2024 | Accepted: 23 March 2024

DOI: 10.1111/cas.16175

ORIGINAL ARTICLE

Cancer Science WILEY

ECM1 and KRT6A are involved in tumor progression and chemoresistance in the effect of dexamethasone on pancreatic cancer

Yoshiki Shinomiya[1,2] | Yusuke Kouchi[1] | Sakurako Harada-Kagitani[1,2] | Takayuki Ishige[3] | Shigetsugu Takano[4] | Masayuki Ohtsuka[4] | Jun-Ichiro Ikeda[2,5] | Takashi Kishimoto[1]

[1]Department of Molecular Pathology, Graduate School of Medicine, Chiba University, Chiba, Japan

[2]Department of Pathology, Chiba University Hospital, Chiba, Japan

[3]Division of Laboratory Medicine, Chiba University Hospital, Chiba, Japan

[4]Department of General Surgery, Graduate School of Medicine, Chiba University, Chiba, Japan

[5]Department of Diagnostic Pathology, Graduate School of Medicine, Chiba University, Chiba, Japan

Correspondence
Takashi Kishimoto, Department of Molecular Pathology, Graduate School of Medicine, Chiba University, 1-8-1 Inohana, Chuo-ku, Chiba 260-8670, Japan.
Email: tkishi@faculty.chiba-u.jp

Abstract

Pancreatic ductal adenocarcinoma (PDAC) has a very poor prognosis. Neoadjuvant chemotherapy is an effective PDAC treatment option, but chemotherapy causes unfavorable side effects. Glucocorticoids (e.g., dexamethasone [DEX]) are administered to reduce side effects of chemotherapy for solid tumors, including pancreatic cancer. Glucocorticoids have both beneficial and detrimental effects, however. We investigated the functional changes and gene-expression profile alterations induced by DEX in PDAC cells. PDAC cells were treated with DEX, and the cell proliferation, migration, invasion, and chemosensitivity to gemcitabine (GEM) were evaluated. The results demonstrated decreased cell proliferative capacity, increased cell migration and invasion, and decreased sensitivity to GEM. A comprehensive genetic analysis revealed marked increases in ECM1 and KRT6A in DEX-treated PDAC cells. We evaluated the effects of ECM1 and KRT6A expression by using PDAC cells transfected with those genes. Neither ECM1 nor KRT6A changed the cells' proliferation, but each enhanced cell migration and invasion. ECM1 decreased sensitivity to GEM. We also assessed the clinicopathological significance of the expressions of ECM1 and KRT6A in 130 cases of PDAC. An immunohistochemical analysis showed that KRT6A expression dominated the poorly differentiated areas. High expressions of these two proteins in PDAC were associated with a poorer prognosis. Our results thus demonstrated that DEX treatment changed PDAC cells' functions, resulting in decreased cell proliferation, increased cell migration and invasion, and decreased sensitivity to GEM. The molecular mechanisms of these changes involve ECM1 and KRT6A, whose expressions are induced by DEX.

KEYWORDS
dexamethasone, ECM1, GEM resistance, KRT6A, pancreatic cancer

Abbreviations: BP, biological process; CC, cellular component; cDNA, complementary DNA; DEG, differentially expressed gene; DEX, dexamethasone; FBS, fetal bovine serum; FFPE, formalin-fixed paraffin-embedded; GEM, gemcitabine; GO, gene ontology; IHC, immunohistochemistry, pancreatic ductal adenocarcinoma; PDAC, pancreatic ductal adenocarcinoma; SDS-PAGE, sodium dodecyl sulfate-polyacrylamide gel electrophoresis.

1 | INTRODUCTION

Pancreatic ductal adenocarcinoma (PDAC) is a highly aggressive cancer with a poor 5-year survival rate of approximately 10%.[1] Therefore, a multidisciplinary approach is indicated in many cases.[2] Neoadjuvant chemotherapy has recently been considered an effective treatment option for resectable, borderline resectable, and locally advanced PDAC.[3] Although chemotherapy has benefits for patients, it also has unfavorable side effects, including nausea, vomiting, diarrhea, fatigue, and fever.[4]

A glucocorticoid is a steroid hormone that has important biological functions in regulating the human body's metabolism, immune response, and stress response.[5-7] The immunomodulatory and anti-inflammatory properties of glucocorticoids can alleviate the side effects of chemotherapy for patients with solid tumors,[8] and synthetic steroids such as dexamethasone (DEX) are thus widely used in conjunction with neoadjuvant chemotherapy for PDAC to help manage various side effects and improve treatment outcomes. Although the pharmacological benefits of glucocorticoids are significant, it is important that clinicians be aware that glucocorticoids might directly affect the phenotype in various types of solid tumors, including breast cancer,[9] ovarian cancer,[10] lung cancer,[11] and pancreatic cancer.[12-15]

In the present study, we used RNA sequencing (RNA-seq) to examine the changes in molecular expressions induced by DEX treatment of PDAC cells. We report that two highly induced molecules, KRT6A and ECM1, are involved in the progression of PDAC.

2 | MATERIALS AND METHODS

2.1 | Cell culture and dexamethasone treatment

Both HPAC cells and the PCI6 cell line were derived from human pancreatic ductal adenocarcinoma. HPAC cells were purchased from the American Type Culture Collection (Rockville, MD, USA). The PCI6 cells were a kind gift from Professor Takashi Yoshiki, Hokkaido University (Hokkaido, Japan). The HPAC cells were cultured in D-MEM/Ham's F-12 medium (FujiFilm Wako, Osaka, Japan) and the PCI6 cells were cultured in RPMI-1640 (FujiFilm Wako), both with 100 U/mL penicillin, 100 μg/mL streptomycin (Thermo Fisher Scientific, Waltham, MA), and 10% FBS (Thermo Fisher Scientific) in a humidified incubator at 37°C and 5% CO_2. Each cell line was treated with DEX at a final concentration 1×10^{-6} mol/L for ≥2 weeks, and control cells were treated with 0.1% ethanol vehicle for the same period.

2.2 | Gene transduction

Lenti-X Packaging Single Shots (VSV-G) (TaKaRa Bio, Shiga, Japan) were used to transfect Lenti-X 293T cells (TaKaRa Bio) with pLV(Exp)-EGFP/Neo-EF1A empty vector, pLV(Exp)-EGFP/Neo-EF1A-hKRT6A vector, and pLV(Exp)-EGFP/Neo-EF1A-hECM1 vector, according to the manufacturer's instructions. The viral titers of the recombinant lentivirus suspensions were determined using the QuickTiter Lentivirus Titer Kit (Lentivirus-Associated HIV p24) (Cell Biolabs, San Diego, CA). The cell lines were infected with these lentiviral preparations with the use of the ViraDuctin Lentivirus Transduction Kit (Cell Biolabs). Stably transduced cells were selected and maintained in complete culture medium supplemented with 800 μg/mL of G418 disulfate salt solution (Sigma-Aldrich, St. Louis, MO).

2.3 | Clinical samples

We analyzed 130 consecutive cases of patients whose PDAC was treated with surgery at Chiba University Hospital from January 2015 to December 2018. None of the patients had received neoadjuvant chemotherapy and, therefore, no patients received preoperative steroids. The formalin-fixed paraffin-embedded (FFPE) surgical specimens used for the present histological examinations and the patients' clinicopathological data were obtained from the digital archives retrospectively. Ethical approval for this study was received from the Institutional Review Board of Chiba University Graduate School of Medicine (approval no. M10061), and the study was performed in accordance with the Declaration of Helsinki.

2.4 | Immunohistochemistry

We performed an immunohistochemistry (IHC) analysis of the FFPE sections using the EnVision Flex system (Agilent Technologies, Santa Clara, CA) according to the manufacturer's instructions. First, the FFPE sections were deparaffined and rehydrated, and then antigen retrieval was performed by heating the sections in citrate buffer (pH 6.0) at 97°C for 20 min. Endogenous peroxidase in the tissue was blocked by a ready-to-use peroxidase blocking solution. Then, anti-ECM1 antibody (dilution 1:500, Merck, Darmstadt, Germany) or anti-cytokeratin 6A antibody (dilution 1:200, Proteintech, Rosemont, IL) was applied and the sections were incubated at room temperature for 30 min. HRP-polymer secondary antibodies were incubated at room temperature for 30 min. The labeled antigen was visualized by 3,3′-diaminobenzidine.

The IHC results were assessed semi-quantitatively with the use of the H-score.[16,17] For the survival analysis, a high expression of ECM1 was defined as an H-score ≥5, and a low ECM1 expression was defined as an H-score <5. High KRT6A expression was defined as an H-score ≥100, and low expression was defined as an H-score <100. For each case in one of the high-expression groups, we evaluated the protein expression in the gland-forming component (57 for ECM1, 55 for KRT6A) and the non-gland-forming component (57 for ECM1, 55 for KRT6A) as positive or negative. The differences in the protein expression between two components were also evaluated.

2.5 | Western blotting

The cell lysate extracted from cultured cells was boiled with 2× sample buffer at 99°C for 5 min. Samples and marker proteins were separated by sodium dodecyl sulfate-polyacrylamide gel electrophoresis (SDS-PAGE) and transferred to polyvinylidene difluoride (PDVF) membranes (Merck). The PDVF membrane with transferred proteins was subsequently blocked by TBST (tris-buffered saline + Polysorbate 20) with 5% skimmed milk at room temperature for 1 h. The blots were then reacted overnight at 4°C with the appropriate primary antibodies diluted in blocking buffer.

The primary antibodies used for the western blotting were anti-ECM1 (Merck), cytokeratin 6A (Proteintech), and β-actin (Merck). After being washed with TBST three times, the blots were incubated with HRP-conjugated secondary antibodies at room temperature for 2 h and then washed another three times with TBST. The proteins bands were detected using a chemiluminescence reagent (Cell Signaling Technology, Beverly, MA).

2.6 | RNA-Seq

Total RNA was isolated from cell lines using the RNeasy Mini Kit (Qiagen), and mRNA was isolated and purified using the Dynabeads mRNA DIRECT Micro Kit (Thermo Fisher Scientific) following the manufacturers' protocols. The Ion Total RNA-Seq Kit v2 for Whole Transcriptome Libraries (Thermo Fisher Scientific) was used for the cDNA library preparation following the manufacturer's procedure. The quality assessment of the library was based on the concentration identified with a Quantus fluorometer (Promega, Madison, WI). The High Sensitivity DNA Kit (Agilent Technology) was used with an Agilent 2100 Bioanalyzer Instrument (Agilent Technology) for the size measurements. Each library was used to perform an emulsion polymerase chain reaction (PCR) and sequenced on an Ion PGM System (Thermo Fisher Scientific). Torrent Suite software (Thermo Fisher Scientific) was used for the gene expression analysis, and the analysis of differentially expressed genes was performed using R ($p < 0.01$, fold change >2.0 or fold change <2.0). The R package clusterProfiler was used for the gene ontology analyses of differentially expressed genes.

2.7 | Reverse transcription-quantitative PCR

Total RNA was isolated from the cultured cells with the RNeasy Mini Kit (Qiagen) according to the recommended protocol. The sample RNA was reversed to cDNA using SuperScript II Reverse Transcriptase (Thermo Fisher Scientific) following the manufacturer's instructions. The reverse transcription quantitative PCR (RT-qPCR) was performed with Power SYBR Green Master Mix (Thermo Fisher Scientific) on an Applied Biosystems 7300 Real Time PCR System (Thermo Fisher Scientific). The RT-qPCR protocol was as follows: initialization at 95°C for 10 min, 40 cycles at 95°C for 15 s, and 60°C for 60 s, and one cycle at 95°C for 15 s, 60°C for 60 s, 95°C for 15 s, and 60°C for 15 s for the melting curve analysis. Each sample was run in triplicate. Relative RNA expression levels of target genes were calculated using the ΔΔCt method.

The primers used in the study were as follows: ECM1, forward primer 5′-CAAATCTGCCTTCCTAACCG-3′ and reverse primer 5′-AAGCAGGAGAACCGAGCC-3′; KRT6A, forward primer 5′-TCACCGTCAACCAGAGTCTC-3′ and reverse primer 5′-GAACCTTGTTCTGCTGCTCC-3′; and GAPDH, forward primer 5′-CAATGACCCCTTCATTGACC-3′ and reverse primer 5′-GATCTCGCTCCTGGAAGATG-3′.

2.8 | Cell proliferation assay

We used the Cell Counting Kit-8 (Dojindo, Mashiki, Japan) to evaluate the cell viability. The cells were seeded in 96-well culture plates at the appropriate concentration (HPAC: 1.2×10^4/mL, PCI6: 3×10^3/mL), and both cell lines were cultured for 72 and 96 h. After cell culture, 10 μL of Cell Counting Kit-8 solution was added to each well and incubated at 37°C for 2 h. The absorbance was measured at OD 450 nm.

2.9 | Gemcitabine resistance assay

Chemoresistance was examined for gemcitabine (GEM), which is commonly used for the patients with pancreatic cancer, especially in NAC. Cultured cells adjusted to the appropriate concentration (HPAC: 1.2×10^4/mL, PCI6: 3×10^3/mL) were seeded in 96-well plates, precultured overnight, and then treated with GEM at graded concentrations for 72 h. After the GEM treatment, the viable cells were measured using the Cell Counting Kit-8, and the survival rate of the cells treated with each concentration of GEM was calculated.

2.10 | Transwell assay for migration and invasion

Transwell assays were performed using the CytoSelect 24-well Cell Migration and Invasion Assay (8 μm) Colorimetric Combo Kit (Cell Biolabs). The cell lines were precultured overnight in serum-free medium. Then, 300 μL of the cell suspension (0.5×10^6 cells/mL) was loaded into the upper chamber, and 500 μL of medium with 10% FBS was added to the lower wells. The cells were incubated at 37°C for 12 h. For the invasion assay, an extracellular matrix (ECM)-coated cell culture insert was used. The cells were incubated at 37°C for 30 h (HPAC) or 48 h (PCI6). After the removal of non-migratory cells, the migrated cells were stained and the pigments on cells were extracted. Each sample was measured at OD 560 nm.

2.11 | Wound-healing assay

A cell suspension (1.0×10^6/mL) was applied into each insert of a Culture-Insert 2 Well 24 (ibidi, Martinsried, Germany) and incubated. When the cells were confluent, the insert was removed to make a cell-free space (the wound), and the medium was replaced with culture medium with 1% FBS to minimize cell growth during the assay. The wound area was measured by Image J software, and the cell migration capacity was evaluated by calculating the percentage of wound closure: Closure rate (%) = The wound area at N h/The wound area at 0 h × 100.

2.12 | Statistical analysis

The experimental data are presented as the mean ± standard deviation (SD). The data distribution between the two groups was compared by Welch's *t*-test, χ^2-test, or a one-way analysis of variance (ANOVA). Kaplan–Meier curves were drawn for the survival analysis, and significant differences in the curves were detected by the log-rank test. The Cox proportional hazard model was used for univariate and multivariate analyses. In all analyses, *p*-values <0.05 were considered significant. R (4.1.2) software was used for the statistical analyses, and the image analysis was carried out using Image J (1.53a).

3 | RESULTS

3.1 | Dexamethasone changed biological functions of pancreatic ductal adenocarcinoma

To examine the direct effects of DEX on pancreatic cancer cells, we cultured HPAC and PCI6 cells in medium containing DEX. Exposure to DEX reduced the cell proliferation by 0.8-fold for the HPAC cells and 0.6-fold for the PCI6 cells compared to their respective controls (Figure 1A). For the examination of the cells' migration capacity, we conducted a wound-healing assay and Transwell assay. In the wound-healing assay, the migration capacity of both HPAC and PCI6 cells was increased in the DEX-treated cells compared to each control, with significant differences in the calculated wound closure rates (Figure 1B). The increased migration of HPAC and PCI6 cells by DEX treatment was also observed in the Transwell assay (Figure 1C). The invasive capacity was increased in PCI6 cells but not in HPAC cells (Figure 1D).

Our assessment of the changes in sensitivity to GEM, which is widely used in chemotherapy for pancreatic cancer, revealed that the DEX-treated HPAC and PCI6 cells had higher survival rates than control cells in the culture medium with titrated concentrations of GEM (Figure 1E).

3.2 | Identification of the altered expressed genes in DEX-treated pancreatic ductal adenocarcinoma cells with the gene expression profile

DEX changed the following functions of both HPAC and PCI6 cells: cell proliferation, migration, invasion, and GEM resistance. To extract molecules that have a potential association with the changed functions in the DEX-treated cells, we conducted a comprehensive mRNA expression analysis of HPAC cells; the results demonstrated that 122 genes were differentially expressed, in which 32 genes were upregulated and 90 genes were downregulated, in DEX-treated HPAC cells compared to control cells (Figure 2A; Table 1).

To identify functional annotations and enriched pathways among these differentially expressed genes (DEGs), we performed a gene ontology (GO) analysis. We observed that the DEGs were enriched mainly in wound healing and in epithelial cell proliferation as a biological process (BP) (Figure 2B) and in collagen-containing extracellular matrix as a cellular component (CC) (Figure 2C). The most highly upregulated mRNA in DEX-treated cells was ECM1, which is one of a collagen-containing extracellular matrix gene. The second most highly upregulated mRNA was KRT6A, which is a gene in the wound-healing gene group. The increased expressions of these two mRNAs by DEX were confirmed by RT-qPCR in PCI6 cells as well as in HPAC cells (Figure 2D,E). The production of both ECM1 and KRT6 proteins was also increased by DEX treatment in both cell lines (Figure 2F,G).

3.3 | ECM1 contributed to enhanced cell migration and invasion and gemcitabine resistance

Because we observed that the ECM1 mRNA expression was upregulated to the greatest degree by DEX in HPAC cells, we overexpressed ECM1 in PDAC cells to evaluate the functional impact of ECM1. HPAC and PCI6 cells transduced with ECM1 by lentiviral vectors exhibited increased mRNA expression and increased protein production of ECM1 (Figure 3A,B). No obvious change in the cells' proliferative capacity was observed with ECM1 transduction in HPAC cells or PCI6 cells (Figure 3C). The wound-healing assays showed that the migration of HPAC and PCI6 cells was significantly increased by ECM1 overexpression (Figure 3D). Increased migration by ECM1 overexpression was also obtained in the Transwell assay for both cell lines (Figure 3E). Overexpression of ECM1 increased the cell invasion of PCI6 cells, but no significant increase was observed in HPAC cells (Figure 3F). Compared to the control cells, the ECM1-transduced cells were more resistant to GEM in both cell lines (Figure 3G). These results revealed that the overexpression of ECM1 partially recapitulated the changes in biological functions altered by DEX treatment.

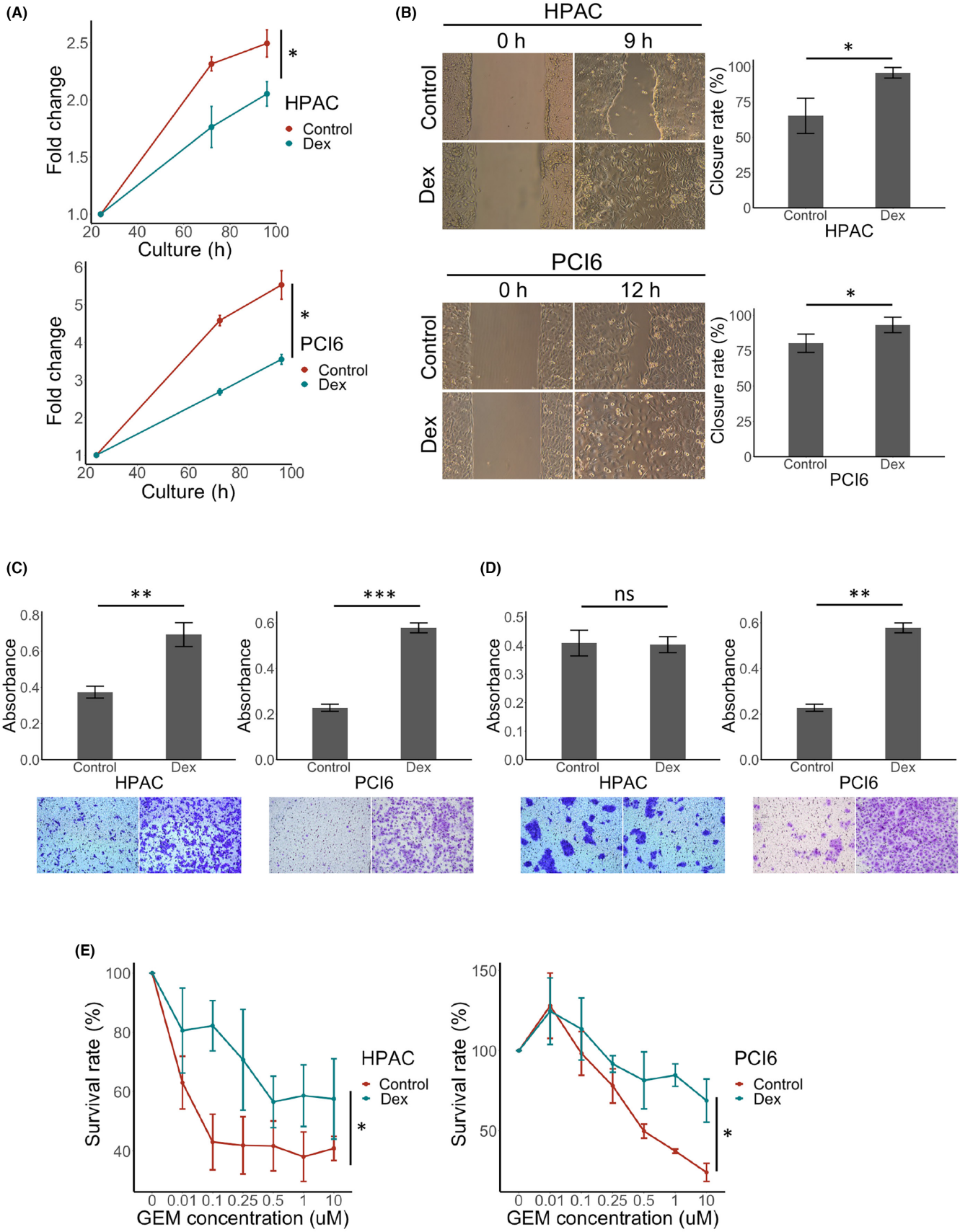

FIGURE 1 Evaluation of the cellular functions of DEX-treated PDAC cells, HPAC cells, and PCI6 cells. (A) Cell proliferation assay. Absorbance was measured at 72 and 96 h after cell seeding. (B) Wound-healing assay. The endpoints for the HPAC and PCI6 cells were 9 and 12 h, respectively, (C) in a migration assay using Transwell. (D) Invasion assay using Transwell. (E) GEM resistance assay. Cell viability was measured after 72 h exposure to graded concentrations of GEM. All assays were performed in triplicate. *$p < 0.05$, **$p < 0.01$, ***$p < 0.001$, ns: no significance.

3.4 | KRT6A promoted cell migration and invasion

To investigate the functions of KRT6A, the second most upregulated by DEX exposure, we performed KRT6A gene transduction into HPAC and PCI6 cells using lentiviral vectors. The stable expression of KRT6A was confirmed by the results of both the real-time RT-PCR and western blotting (Figure 4A,B). The cell proliferation assay findings revealed that the overexpression of KRT6A induced no significant change of cell proliferation in HPAC or PCI6 cells (Figure 4C). In the wound-healing assay, the migration ability of the KRT6A-transfected cells was significantly increased compared to the control cells in both cell lines (Figure 4D). The increased migration by KRT6A overexpression was confirmed by the Transwell assay results in both cell lines (Figure 4E). For the invasion assay, there was no significant difference between the KRT6A-transfected cells and control cells in the HPAC cell line, but in the PCI6 cells, significantly increased invasion occurred due to KRT6A overexpression (Figure 4F). There were no significant changes in GEM resistance by KRT6A overexpression in either HPAC or PCI6 cells (Figure 4G). These results revealed that the overexpression of KRT6A, as well as that of ECM1, partially recapitulated the changes in the cells' biological functions altered by DEX exposure.

3.5 | Association of ECM1 expression and KRT6A expression with tumor histopathology

The immunohistochemistry analyses using ECM1 and KRT6A were performed with the samples from patients with PDAC, and the association between the protein expression and morphology was assessed. Both ECM1 (Figure 5A–C) and KRT6A (Figure 5D–F) were expressed on the cell membrane and/or cytoplasm of the PDAC cells. ECM1 expression localized to the luminal surface of the glandular ducts was also observed in the well-differentiated areas (Figure 5A). Our comparison of the protein expression between the well-to-moderately differentiated areas showing tubular/glandular structures, and the poorly differentiated areas without tubular/glandular structures demonstrated that KRT6A was significantly more highly expressed in the poorly differentiated areas ($p = 0.0145$) (Figure 5G). Interestingly, some cases showed strong positivity selectively in the budding clusters (Figure 5H). KRT6A was also positive in cells showing morphological squamous differentiation (Figure 5I). Conversely, ECM1 was more frequently expressed in well-differentiated tube-forming clusters ($p < 0.0001$) (Table S1).

3.6 | The clinicopathologic significance of ECM1 and KRT6A in pancreatic ductal adenocarcinoma patients

To examine the clinicopathological significance of the expression of ECM1 and that of KRT6A, we divided the patients into high- and low-expression groups. High expression of ECM1 was observed in 57/130 cases, and high expression of KRT6A was identified in 56/130 cases. Between the ECM1 high- and low-expression groups, there was no significant association of age, sex, histological differentiation, pathological stage, tumor size, lymphatic metastasis, tumor location, medical history, complications of diabetes, postoperative adjuvant chemotherapy, and DEX administration or curative resection (Table S2). Similarly, no association with clinicopathological factors, except for sex, was observed in the KRT6A high- and low-expression groups (Table S3). There was a significant correlation between ECM1 and KRT6A expression ($p = 0.013$) (Tables S2 and S3).

Follow-up data were available for 130 cases, and the median follow-up of the total series of patients was 25.35 months (range 0.8–83.5 months). The comparison of the prognoses of the high- and low-expression groups showed that the patients' overall survival (OS) was significantly shorter in the high-expression group for both ECM1 and KRT6A (Figure 6A,C). However, the patients' disease-free survival (DFS) showed no significant difference between the two expression groups for either ECM1 or KRT6A (Figure 6B,D). In addition, to validate these results, a prognostic analysis was performed using publicly available data from The Cancer Genome Atlas (TCGA, Pancreatic Adenocarcinoma, PanCancer Atlas, $n = 177$) on cBioPortal. In this validation analysis, the expressions of ECM1 and KRT6A were statistically significant poor prognostic factors for both OS and progression-free survival (PFS) (Figure S1). We further analyzed the prognoses by dividing the patients into four groups: those with high expressions of both proteins, those with a high expression of either ECM1 or KRT6A, and those with a low expression of both proteins. There was no clinicopathologically significant difference among the four groups (Table S4).

The groups with high expressions of both proteins had the poorest OS and DFS, followed by those with a high expression of only ECM1 or KRT6A and those with low expressions of both proteins (Figure 6E,F). The results of the univariate and multivariate Cox regression analyses for OS and DFS are provided in Tables 2 and 3. In the univariate analysis, the high expression of both ECM1 and KRT6A was significantly associated with a worse OS ($p = 0.0007$) and a worse DFS ($p = 0.0361$). The multivariate analysis revealed that the high expression of both ECM1 and KRT6A was an independent prognostic factor for the patients' OS and DFS.

FIGURE 2 The detection of differentially expressed genes (DEGs) and the extraction of candidate genes (A) in a volcano plot. The results of the RNA-Seq for HPAC cells are plotted. (B) The dot plot of the gene ontology (GO) analysis (Bio process) (C) The dot plot of the GO analysis (cell component) results. (D) The real-time PCR results. The ECM1 mRNA levels were measured. (E) The real-time PCR results; the mRNA levels of KRT6A. (F) Western blotting for ECM1. The band of β-actin was confirmed as the endogenous control. (G) Western blotting for KRT6A.

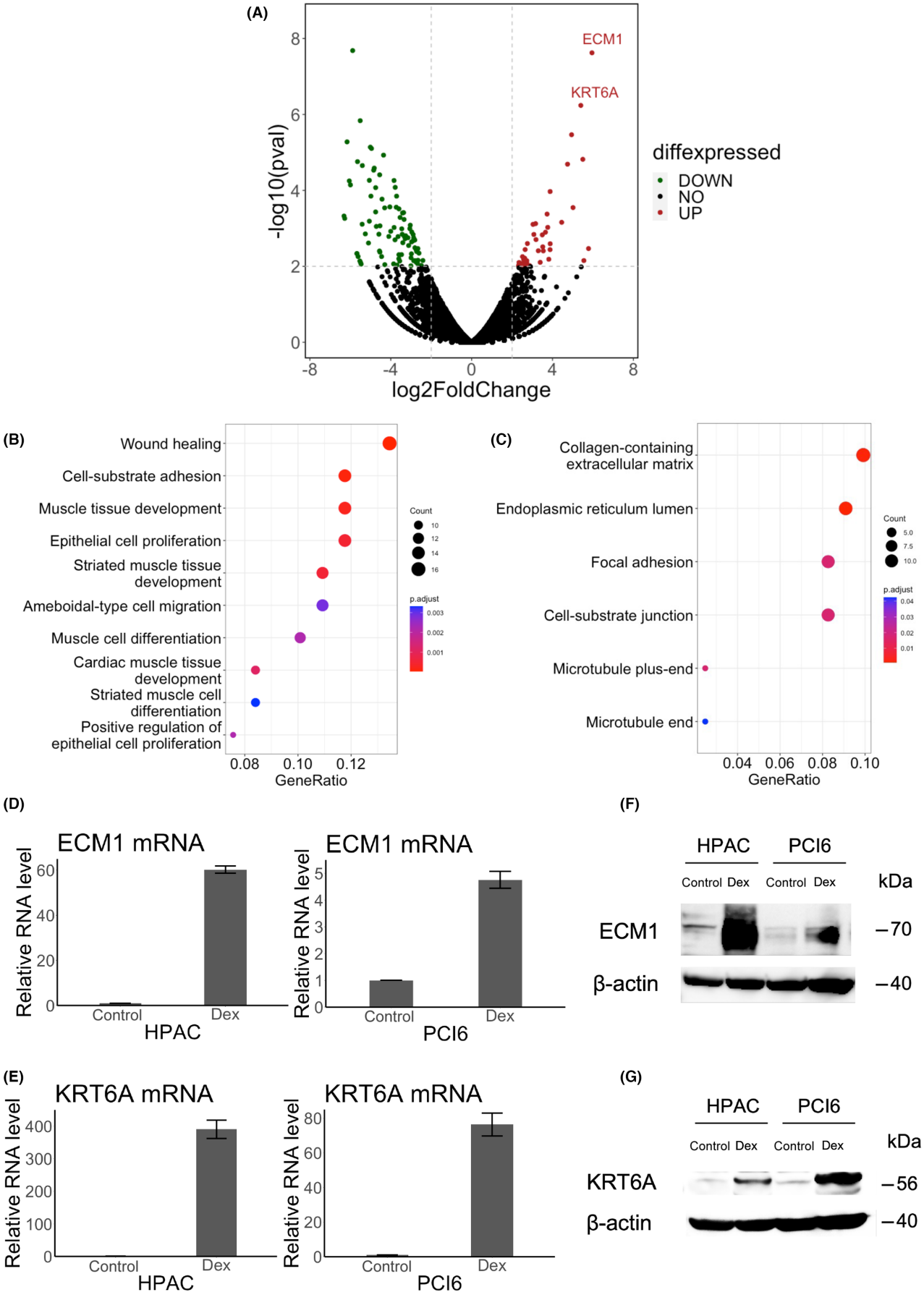
(A)
ECM1
KRT6A
-log10(pval)
log2FoldChange
diffexpressed
DOWN
NO
UP
(B)
Wound healing
Cell-substrate adhesion
Muscle tissue development
Epithelial cell proliferation
Striated muscle tissue development
Ameboidal-type cell migration
Muscle cell differentiation
Cardiac muscle tissue development
Striated muscle cell differentiation
Positive regulation of epithelial cell proliferation
GeneRatio
Count
p.adjust
(C)
Collagen-containing extracellular matrix
Endoplasmic reticulum lumen
Focal adhesion
Cell-substrate junction
Microtubule plus-end
Microtubule end
GeneRatio
Count
p.adjust
(D)
ECM1 mRNA
Relative RNA level
Control
Dex
HPAC
ECM1 mRNA
Relative RNA level
Control
Dex
PCI6
(F)
HPAC
PCI6
Control Dex Control Dex
kDa
ECM1
β-actin
70
40
(E)
KRT6A mRNA
Relative RNA level
Control
Dex
HPAC
KRT6A mRNA
Relative RNA level
Control
Dex
PCI6
(G)
HPAC
PCI6
Control Dex Control Dex
kDa
KRT6A
β-actin
56
40

TABLE 1 Thirty-two upregulated DEGs.

Gene symbol	Gene name	Fold change	*p*-value
ECM1	Extracellular matrix protein 1	61.8880097	2.38E-08
KRT6A	Keratin 6A	42.2562066	5.79E-07
A2ML1	Alpha-2-macroglobulin like 1	30.7512865	3.42E-06
PTGS2	Prostaglandin-endoperoxide synthase 2	26.7816712	2.04E-05
FKBP5	FKBP prolyl isomerase 5	14.7396226	1.07E-04
GABRP	Gamma-aminobutyric acid type A receptor subunit pi	32.3490566	2.84E-04
HOPX	HOP homeobox	13.2860377	4.21E-04
DNER	Delta/notch like EGF repeat containing	21.9056604	6.94E-04
DHRS9	Dehydrogenase/reductase 9	8.95489387	7.51E-04
KRT13	Keratin 13	8.19788999	7.85E-04
HPGD	15-hydroxyprostaglandin dehydrogenase	13.5849057	9.42E-04
RASSF2	Ras association domain family member 2	12.5448113	0.00126636
EFNB1	Ephrin B1	8.43794845	0.00144625
TFCP2L1	Transcription factor CP2 like 1	11.2584906	0.00148362
ASS1	Argininosuccinate synthase 1	6.76239773	0.00250989
FLRT3	Fibronectin leucine rich transmembrane protein 3	14.7735849	0.00254277
TSC22D3	TSC22 domain family member 3	11.4426705	0.00305891
MGAM	Maltase-glucoamylase	55.0188679	0.00340365
DDIT4	DNA damage inducible transcript 4	6.25876011	0.00361843
SCNN1B	Sodium channel epithelial 1 subunit beta	14.7008086	0.00363603
SP6	Sp6 transcription factor	9.8290788	0.00388806
FXYD3	FXYD domain containing ion transport regulator 3	5.7202809	0.0055664
ADAMTSL4	ADAMTS like 4	14.0943396	0.00651051
ACADM	Acyl-CoA dehydrogenase medium chain	5.95471698	0.00666806
SLC16A9	Solute carrier family 16 member 9	46.8679245	0.00705532
MUC16	Mucin 16, cell surface associated	10.4943396	0.00784447
GLUL	Glutamate-ammonia ligase	5.07073651	0.00793291
PHACTR3	Phosphatase and Actin regulator 3	5.4588127	0.00845712
MAOA	Monoamine oxidase A	6.51539225	0.0087633
FAM83A	Family with sequence similarity 83 member A	5.01363721	0.00942804
GTF2A2	General transcription factor IIA subunit 2	5.78975741	0.0095344
PITX1	Paired like homeodomain 1	5.02437444	0.00989287

Note: Pseudogenes were excluded from the list.

4 | DISCUSSION

The results of our analyses demonstrated that DEX treatment inhibited the proliferation of pancreatic cancer cells, increased their migration and invasive potential, and decreased their sensitivity to gemcitabine, a chemotherapeutic agent used in the treatment of pancreatic cancer. The most important aspect of this study was the comprehensive examination of DEX-induced changes in gene expression; we found that the two most highly expressed genes, ECM1 and KRT6A, had important roles in the DEX-induced functional changes of pancreatic cancer cells.

FIGURE 3 Functional evaluation of ECM1-transduced cells. (A) The relative levels of ECM1 mRNA. (B) Western blots for ECM1. Bands can be seen in the transduced cells. (C) The cell proliferation assay. The data in the plots represent absorbance at 72 and 96 h after cell seeding. (D) Wound-healing assay. The closure rate was calculated after measuring the wound area at 9 h for HPAC cells and at 12 h for PCI6 cells. (E) The cell migration assay using a Transwell. (F) The invasion assay using a Transwell. (G) The GEM resistance assay. All assays were performed in triplicate. $^{*}p < 0.05$, $^{**}p < 0.01$, ns: no significance.

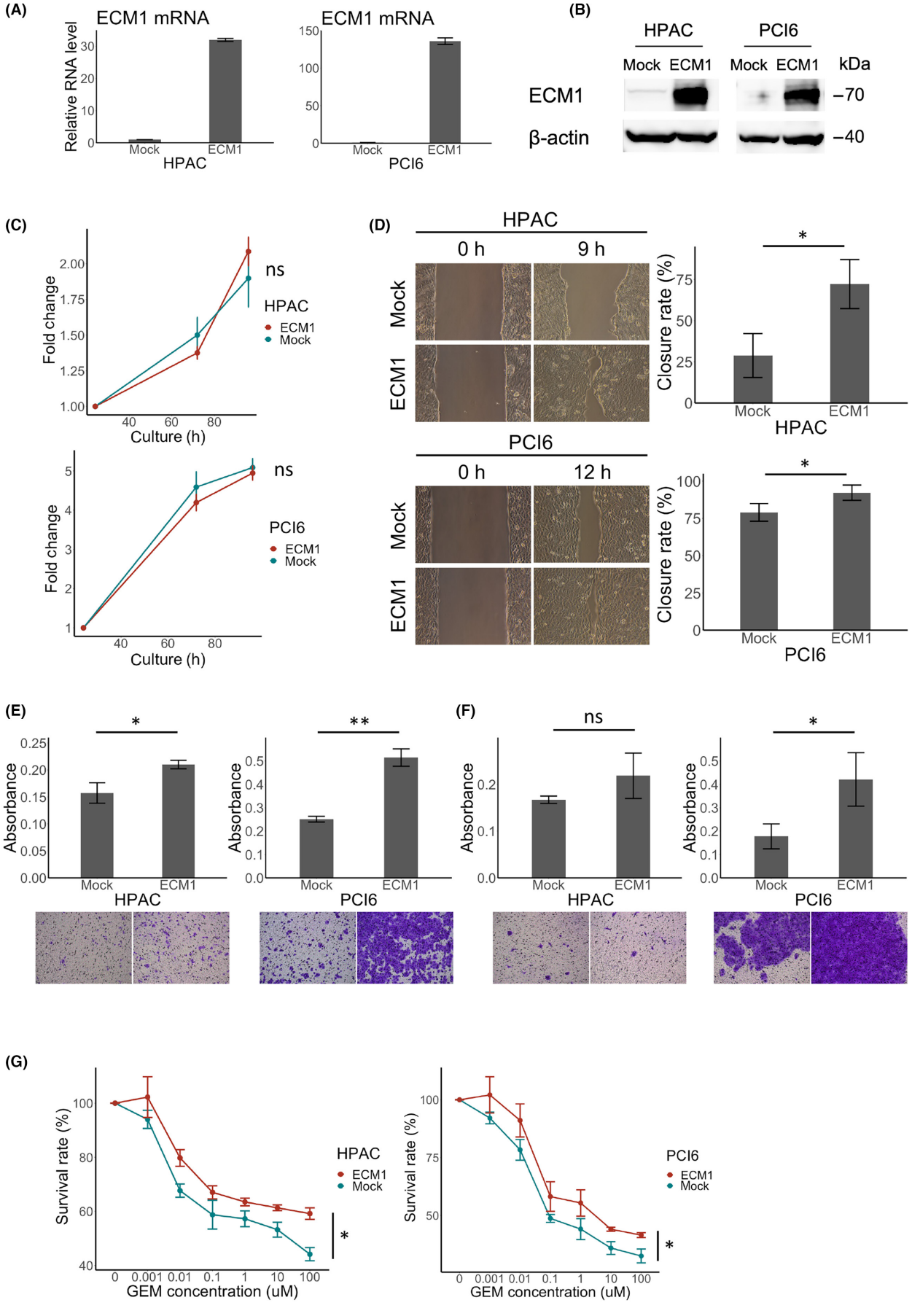
(A)
ECM1 mRNA
Relative RNA level
Mock
ECM1
HPAC
PCI6
(B)
HPAC
PCI6
Mock ECM1 Mock ECM1 kDa
ECM1
β-actin
−70
−40
(C)
Fold change
Culture (h)
ns
HPAC
ECM1
Mock
PCI6
(D)
HPAC
0 h
9 h
Mock
ECM1
Closure rate (%)
PCI6
12 h
(E)
Absorbance
(F)
ns
*
**

(G)
Survival rate (%)
GEM concentration (uM)
HPAC
PCI6
ECM1
Mock

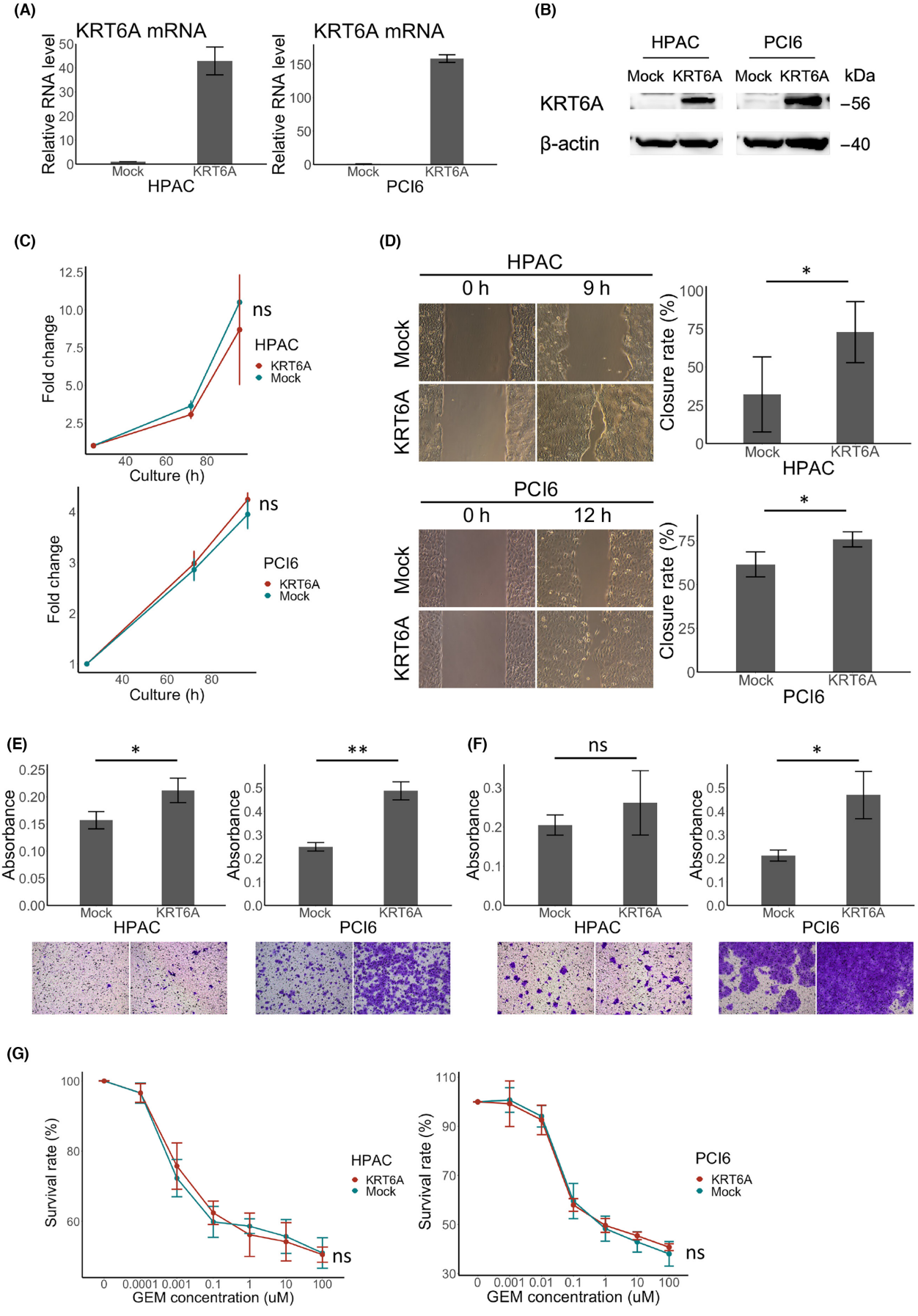
(A)
KRT6A mRNA
Relative RNA level
Mock
KRT6A
HPAC
PCI6
(B)
HPAC
PCI6
Mock KRT6A Mock KRT6A kDa
KRT6A
β-actin
–56
–40
(C)
Fold change
Culture (h)
ns
HPAC
KRT6A
Mock
PCI6
(D)
HPAC
0 h
9 h
Mock
KRT6A
Closure rate (%)
*
PCI6
0 h
12 h
(E)
Absorbance
*
**
(F)
ns
*
(G)
Survival rate (%)
GEM concentration (uM)
HPAC
PCI6
ns

FIGURE 4 Evaluation of cellular function for KRT6A-transducted cells. (A) The relative mRNA levels of KRT6A. (B) Western blots for KRT6A. (C) Cell proliferation assay. Absorbance was measured at 72 and 96 h after cell seeding. (D) Wound-healing assays. The endpoints for HPAC and PCI6 cells were 9 and 12 h, respectively. (E) The migration assay using a Transwell. (F) The invasion assay using Transwell. (G) The GEM resistance assay. All assays were performed in triplicate. $^{*}p < 0.05$, $^{**}p < 0.01$, ns: no significance.

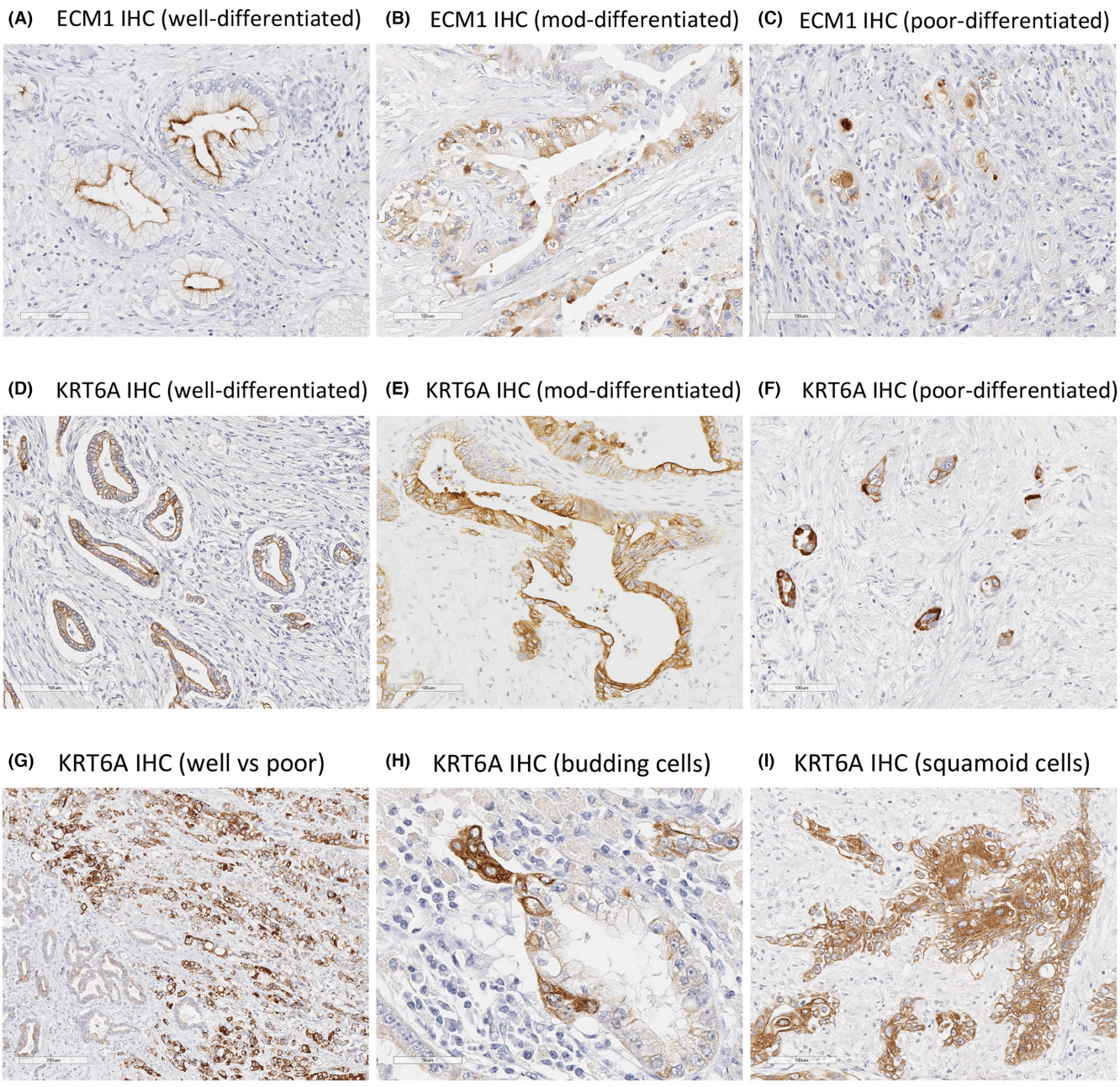

FIGURE 5 Immunohistochemistry (IHC) analyses of surgical specimens from patients with pancreatic ductal adenocarcinoma (PDAC). (A) The ECM1 IHC for well-differentiated components. (B) The ECM1 IHC for moderately differentiated components. (C) The ECM1 IHC for poorly differentiated components. (D) The KRT6A IHC for well-differentiated components. (E) The KRT6A IHC for moderately differentiated components. (F) The KRT6A IHC for poorly differentiated components. (G) Contrast in staining intensity of KRT6A IHC between well-differentiated and poorly differentiated components within the same case. (H) Budding cells stained for KRT6A. (I) Squamoid cells stained for KRT6A.

ECM1 is a gene that encodes a protein known as extracellular matrix protein 1. The expression of ECM1 has been implicated in the promotion of tumor progression and metastasis in various types of cancer.[18–22] ECM1 was reported to promote the proliferation and invasion of PDAC cells, and the high expression of ECM1 was reported to be associated with poor prognosis[23,24]; these reports are consistent with our present findings. However, in our study high ECM1 expression did not affect the

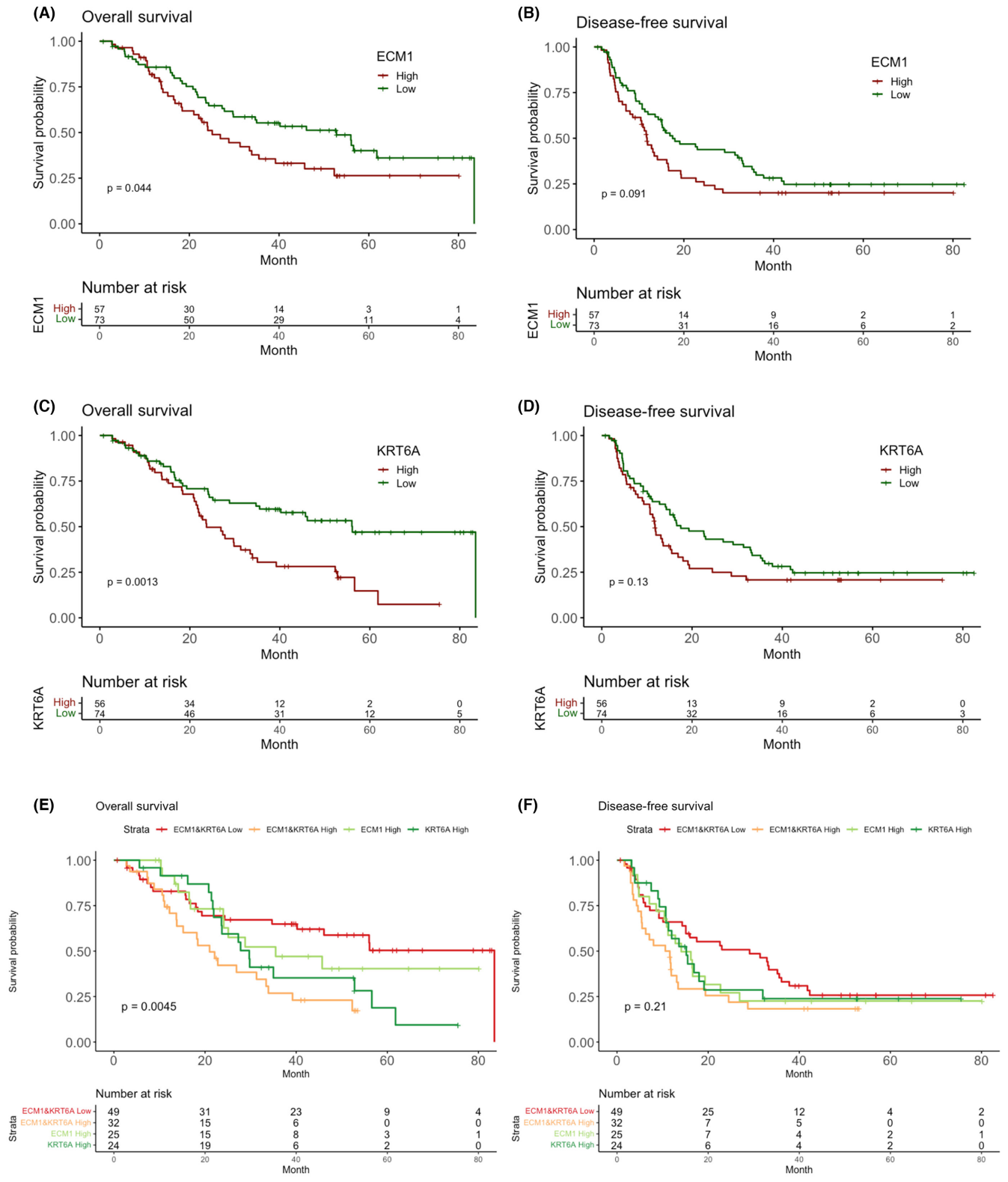

FIGURE 6 Kaplan–Meier curves of the cases with high- or low-expression of ECM1 and KRT6A. The overall survival (OS) (A) and disease-free survival (DFS) (B) of the patients with high and low expressions of ECM1. The OS (C) and DFS (D) of the patients with high and low expressions of KRT6A. The OS (E) and DFS (F) of the patients with a high expression of both ECM1 and KRT6A; the patients with a high expression of either ECM1 or KRT6A and the patients with low expression of both ECM1 and KRT6A.

TABLE 2 Multivariate and univariate analyses of prognostic features in overall survival.

	Multivariate analysis			Univariate analysis		
Parameters	HR	95% CI	*p*-value	HR	95% CI	*p*-value
Age	-	-	-	1.016	0.992–1.042	0.1950
Male	-	-	-	0.894	0.563–1.420	0.6350
ECM1&KRT6A High	2.942	1.537–5.628	**0.0011**	2.893	1.563–5.352	**0.0007**
ECM1 High	1.329	0.637–2.774	0.4500	1.385	0.675–2.842	0.3746
KRT6A High	2.704	1.374–5.320	**0.0040**	1.955	1.019–3.751	**0.0437**
Poorly differentiation	-	-	-	1.427	0.783–2.603	0.2460
pT3–4	2.505	1.184–5.298	**0.0163**	2.584	1.318–5.067	**0.0057**
pN1–2	1.759	0.925–3.343	0.0849	2.495	1.427–4.362	**0.0013**
M	1.511	0.619–3.686	0.3643	3.414	1.546–7.536	**0.0024**
pStage 3 or 4	1.604	0.891–2.886	0.1149	2.448	1.534–3.909	**0.0002**
Vascular invasion	3.455	0.467–25.536	0.2244	8.557	1.185–61.82	**0.0334**
Perineural invasion	6.751	0.894–50.963	0.0641	10.728	1.488–77.33	**0.0185**
Peripancreatic invasion	-	-	-	1.739	0.794–3.806	0.1660
Past medical history: benign tumor	-	-	-	0.816	0.326–2.043	0.664
Past medical history: malignant tumor	-	-	-	1.307	0.724–2.359	0.374
Diabetes	-	-	-	1.508	0.892–2.549	0.126
Adjuvant chemotherapy	-	-	-	0.896	0.559–1.438	0.650
DEX administration (during adjuvant chemotherapy)	-	-	-	0.769	0.280–2.114	0.610

Note: Bold values were used to highlight numbers that were significantly different ($p<0.05$).
Abbreviations: 95% CI, 95% confidence interval; DEX, dexamethasone; HR, hazard ratio.

TABLE 3 Multivariate and univariate analyses of prognostic features in disease free survival.

	Multivariate analysis			Univariate analysis		
Parameters	HR	95% CI	*p*-value	HR	95% CI	*p*-value
Age	-	-	-	1.010	0.990–1.030	0.3410
Male	-	-	-	0.785	0.524–1.176	0.2410
ECM1 & KRT6A High	2.045	1.194–3.503	**0.0091**	1.746	1.037–2.941	**0.0361**
ECM1 High	1.204	0.665–2.181	0.5402	1.265	0.712–2.246	0.4227
KRT6A High	1.711	0.931–3.146	0.0838	1.205	0.671–2.164	0.5333
Poorly differentiation	-	-	-	0.868	0.473–1.593	0.6490
pT3-4	2.820	1.482–5.369	**0.0016**	2.462	1.330–4.555	**0.0041**
pN1-2	2.334	1.324–4.112	**0.0034**	3.085	1.856–5.130	**1.40E-05**
M	1.464	0.655–3.272	0.3529	2.932	1.415–6.078	**0.0038**
pStage3 or 4	1.566	0.943–2.602	0.0830	2.498	1.649–3.786	**1.58E-05**
Vascular invasion	-	-	-	2.557	0.938–6.972	0.0667
Perineural invasion	3.300	0.990–10.998	0.0520	5.096	1.610–16.130	**5.61E-03**
Peripancreatic invasion	-	-	-	1.718	0.889–3.320	0.1070
Past medical history: benign tumor	-	-	-	1.064	0.512–2.213	0.868
Past medical history: malignant tumor	-	-	-	1.128	0.655–1.943	0.664
Diabetes	-	-	-	1.128	0.693–1.836	0.627
Adjuvant Chemotherapy	-	-	-	0.843	0.562–1.266	0.411
DEX administration (during adjuvant chemotherapy)	-	-	-	0.992	0.434–2.268	0.984

Note: Bold values were used to highlight numbers that were significantly different ($p<0.05$).
Abbreviations: 95% CI, 95% confidence interval; DEX, dexamethasone; HR, hazard ratio.

cell proliferative capacity, possibly due to differences in the cell lines used.

KRT6A is a human gene that encodes a protein called keratin 6A. In normal tissues, KRT6A is not expressed in the glandular epithelium. However, it can be expressed in adenocarcinoma, and a high heterotopic expression of KRT6A affects the migratory and invasive potential of cancer cells.[25,26] KRT6A has also been reported by different research groups as a candidate gene in a gene expression signature that is associated with the prognosis and therapeutic resistance in pancreatic cancer.[27,28] Our present survival analysis of PDAC cases also showed a significantly worse prognosis in the high-KRT6A-expression group. In the IHC analysis, KRT6A staining was observed in components suspected of squamous differentiation. Adenosquamous carcinoma is generally considered to have a more unfavorable prognosis than adenocarcinoma,[29] and the prognostic difference identified in the present study might be attributed to the inclusion of cases with squamous differentiation components in the high-KRT6A-expression group. However, many adenocarcinoma cells were also strongly stained. In particular, poorly differentiated components and budding cells tended to be positive. This suggests that KRT6A is strongly involved in cell migration and invasion.

Dexamethasone is known to activate various signaling pathways via glucocorticoid receptors (GRs) expressed on cancer cells,[12,30] and we speculate that the induction of ECM1 and KRT6A by DEX was also triggered by GRs. A complex signaling system involving tumor growth factor-beta (TGFβ) and c-Jun-NH2 terminal kinase-activator protein 1 (JNK/AP-1) was observed to be activated in DEX-treated PDAC cells.[12] In the present study, a TGFβ receptor inhibitor (LY2109761) and a JNK inhibitor (SP600125) incompletely suppressed ECM1 expression by DEX of HPAC and PCI6. KRT6A was also incompletely repressed by both inhibitors to TGFβ receptor and JNK in PCI6 cells but not in HPAC cells (Figure S2). These results suggested that the TGFβ and JNK pathways could be involved, although partially, in the mechanism by which DEX increased ECM1 and KRT6A expression. Furthermore, we suspected the association between the two molecules because both ECM1 and KRT6A were significantly induced by DEX. In the IHC cohort, we observed a correlation between the expression of ECM1 and KRT6A, but there was no induction of KRT6A expression in ECM1-transfected cells and vice versa (data not shown). These results suggested that the ECM1 and KRT6A might be indirectly related through the mediation of some molecules, rather than having a direct interaction.

We observed that overexpression of ECM1 and KRT6A altered pancreatic cancer cell migration, invasion, and gemcitabine sensitivity. It is possible that EMT was induced as a mechanism that caused these changes. There are previous reports of ECM1 or KRT6A promoting EMT in several kinds of cancer cells.[25,31–35] However, we were not able to detect EMT of HPAC cells and PCI6 cells: none of the cell lines overexpressing ECM1 and KRT6A showed reduced expression of E-cadherin or increased expression of vimentin.

The DEX treatment of PDAC cells in this study induced the expressions of ECM1 and KRT6A and promoted cellular functions involved in tumor progression. The PDAC patients with high expressions of both proteins had worse prognoses than the patients with a high expression of only one or neither of these proteins. These results suggest that exposure to DEX might cause pancreatic cancer cell progression in PDAC patients. In contrast, an inhibition of the cells' proliferative potential was observed in this study. Other groups have found that DEX reduced the tumor size in vivo, providing evidence that DEX has an antitumor effect,[36] but if cancer cell migration and invasion are increased, and if cancer cells scattered throughout the body are less sensitive to chemotherapy, the effect of neoadjuvant chemotherapy might be reduced. Indeed, there are several reports that DEX promoted the metastasis and advancement of cancer.[12,13,37,38]

In this study, DEX promoted invasive capacity, migration, and resistance to GEM while simultaneously suppressing proliferative capacity. This duality of effects could potentially be explained by the expression of proliferation-related genes not having been significantly induced by DEX in HAPC and PCI6 cells. In fact, among the DEGs associated with cell proliferation in the GO analysis of RNA-seq for HPAC cells, many of the growth factors were downregulated while many of the growth suppressors were upregulated. Another possibility is that the concentration of DEX might be relevant. It has been reported that the effect of DEX on the growth of breast cancer cells inoculated into mice is concentration dependent (low concentration inhibits and high concentration promotes).[39] The concentration of DEX used in this study is the same as in the previous paper, but it is possible that a higher concentration of DEX in our cell line (HPAC, PCI6) might have a growth-promoting effect.

Unfortunately, our study does not directly demonstrate that PDAC patients are adversely affected by DEX administration. Therefore, we cannot conclude that DEX should not be administered to PDAC patients based on the results of the present study. However, we consider that DEX treatment still has the potential to have adverse effects on patients, and more detailed studies and careful dosing to patients are thus required.

In conclusion, dexamethasone might directly affect pancreatic cancer cells, resulting in a suppression of the cells' proliferative capacity, increased migration and invasion, and increased drug resistance. ECM1 and KRT6A, the expressions of which are upregulated by dexamethasone, are involved in these functional changes, and the expressions of ECM1 and KRT6A affect the prognosis of patients with pancreatic cancer. Dexamethasone is an effective agent in the treatment of patients with pancreatic cancer patients, but it can also have detrimental effects.

AUTHOR CONTRIBUTIONS

Yoshiki Shinomiya: Data curation; formal analysis; investigation; methodology; resources; validation; visualization; writing – original draft. **Yusuke Kouchi:** Conceptualization; validation. **Sakurako Harada-Kagitani:** Conceptualization; methodology; validation. **Takayuki Ishige:** Investigation; supervision. **Shigetsugu Takano:**

Resources; supervision. **Masayuki Ohtsuka:** Resources; supervision. **Jun-Ichiro Ikeda:** Conceptualization; data curation; supervision. **Takashi Kishimoto:** Conceptualization; data curation; project administration; supervision; writing – review and editing.

ACKNOWLEDGMENTS

We thank the technicians of the Department of Molecular Pathology and General Surgery, Chiba University Graduate School of Medicine for their excellent technical assistance.

FUNDING INFORMATION

This research did not receive any specific grant from funding agencies in the public, commercial, or not-for-profit sectors.

CONFLICT OF INTEREST STATEMENT

The authors have no conflicts of interest directly relevant to the content of this article.

ETHICS STATEMENT

Approval of the research protocol by an Institutional Review Board: The research protocol was approved by the Institutional Review Board of Chiba University.

Informed Consent: N/A.

Registry and the registration no. of the study: Chiba University Registry. no. M10061.

Animal studies: N/A.

ORCID

Yusuke Kouchi https://orcid.org/0000-0002-3434-1263

Shigetsugu Takano https://orcid.org/0000-0002-6495-0422

Takashi Kishimoto https://orcid.org/0000-0002-7552-7259

REFERENCES

1. Siegel RL, Miller KD, Fuchs HE, Jemal A. Cancer statistics, 2022. *CA Cancer J Clin*. 2022;72:7-33.
2. Park W, Chawla A, O'Reilly EM. Pancreatic cancer: a review. *JAMA*. 2021;326:851-862.
3. Springfeld C, Ferrone CR, Katz MHG, et al. Neoadjuvant therapy for pancreatic cancer. *Nat Rev Clin Oncol*. 2023;20:318-337.
4. Aprile G, Rihawi K, De Carlo E, Sonis ST. Treatment-related gastrointestinal toxicities and advanced colorectal or pancreatic cancer: a critical update. *World J Gastroenterol*. 2015;21:11793-11803.
5. Greenhill C. Dexamethasone in patients with diabetes mellitus. *Nat Rev Endocrinol*. 2022;18:333.
6. Giles AJ, Hutchinson MND, Sonnemann HM, et al. Dexamethasone-induced immunosuppression: mechanisms and implications for immunotherapy. *J Immunother Cancer*. 2018;6:51.
7. Snyder JS, Soumier A, Brewer M, Pickel J, Cameron HA. Adult hippocampal neurogenesis buffers stress responses and depressive behaviour. *Nature*. 2011;476:458-461.
8. Gralla RJ, Osoba D, Kris MG, et al. Recommendations for the use of antiemetics: evidence-based, clinical practice guidelines. American Society of Clinical Oncology. *J Clin Oncol*. 1999;17:2971-2994.
9. Ferrand N, Stragier E, Redeuilh G, Sabbah M. Glucocorticoids induce CCN5/WISP-2 expression and attenuate invasion in oestrogen receptor-negative human breast cancer cells. *Biochem J*. 2012;447:71-79.
10. Karlan BY, Jones J, Slamon DJ, Lagasse LD. Glucocorticoids stabilize HER-2/neu messenger RNA in human epithelial ovarian carcinoma cells. *Gynecol Oncol*. 1994;53:70-77.
11. Srivastava S, Siddiqui S, Singh S, et al. Dexamethasone induces cancer mitigation and irreversible senescence in lung cancer cells via damaging cortical Actin and sustained hyperphosphorylation of pRb. *Steroids*. 2023;198:109269.
12. Liu L, Aleksandrowicz E, Schonsiegel F, et al. Dexamethasone mediates pancreatic cancer progression by glucocorticoid receptor, TGFbeta and JNK/AP-1. *Cell Death Dis*. 2017;8:e3064.
13. Abukiwan A, Nwaeburu CC, Bauer N, et al. Dexamethasone-induced inhibition of miR-132 via methylation promotes TGF-beta-driven progression of pancreatic cancer. *Int J Oncol*. 2019;54:53-64.
14. Yao Y, Yao QY, Xue JS, et al. Dexamethasone inhibits pancreatic tumor growth in preclinical models: involvement of activating glucocorticoid receptor. *Toxicol Appl Pharmacol*. 2020;401:115118.
15. Liu L, Han S, Xiao X, et al. Glucocorticoid-induced microRNA-378 signaling mediates the progression of pancreatic cancer by enhancing autophagy. *Cell Death Dis*. 2022;13:1052.
16. Meyerholz DK, Beck AP. Principles and approaches for reproducible scoring of tissue stains in research. *Lab Invest*. 2018;98:844-855.
17. Fedchenko N, Reifenrath J. Different approaches for interpretation and reporting of immunohistochemistry analysis results in the bone tissue - a review. *Diagn Pathol*. 2014;9:221.
18. Han Z, Ni J, Smits P, et al. Extracellular matrix protein 1 (ECM1) has angiogenic properties and is expressed by breast tumor cells. *FASEB J*. 2001;15:988-994.
19. Lopez-Marure R, Contreras PG, Dillon JS. Effects of dehydroepiandrosterone on proliferation, migration, and death of breast cancer cells. *Eur J Pharmacol*. 2011;660:268-274.
20. Lee KM, Nam K, Oh S, et al. Correction to: ECM1 regulates cell proliferation and trastuzumab resistance through activation of EGF-signaling. *Breast Cancer Res*. 2019;21:45.
21. Chen H, Jia WD, Li JS, et al. Extracellular matrix protein 1, a novel prognostic factor, is associated with metastatic potential of hepatocellular carcinoma. *Med Oncol*. 2011;28(Suppl 1):S318-S325.
22. Abdel Salam R, El-Badry N, Rizk A, El-Sedfy A, Kamel N, El-Abd E. Expression of ECM1 and MMP-2 in follicular thyroid lesions among Egyptians. *Cancer Biomark*. 2015;15:441-458.
23. Huang W, Huang Y, Gu J, et al. miR-23a-5p inhibits cell proliferation and invasion in pancreatic ductal adenocarcinoma by suppressing ECM1 expression. *Am J Transl Res*. 2019;11:2983-2994.
24. Li M, Wu P, Yang Z, et al. miR-193a-5p promotes pancreatic cancer cell metastasis through SRSF6-mediated alternative splicing of OGDHL and ECM1. *Am J Cancer Res*. 2020;10:38-59.
25. Yang B, Zhang W, Zhang M, Wang X, Peng S, Zhang R. KRT6A promotes EMT and cancer stem cell transformation in lung adenocarcinoma. *Technol Cancer Res Treat*. 2020;19:1533033820921248.
26. Xu Y, Wang X, Chu Y, et al. Analysis of transcript-wide profile regulated by microsatellite instability of colorectal cancer. *Ann Transl Med*. 2022;10:169.
27. Lu Y, Li D, Liu G, et al. Identification of critical pathways and potential key genes in poorly differentiated pancreatic adenocarcinoma. *Onco Targets Ther*. 2021;14:711-723.
28. Raman P, Maddipati R, Lim KH, Tozeren A. Pancreatic cancer survival analysis defines a signature that predicts outcome. *PloS One*. 2018;13:e0201751.
29. Boyd CA, Benarroch-Gampel J, Sheffield KM, Cooksley CD, Riall TS. 415 patients with adenosquamous carcinoma of the pancreas: a population-based analysis of prognosis and survival. *J Surg Res*. 2012;174:12-19.
30. Cain DW, Cidlowski JA. Immune regulation by glucocorticoids. *Nat Rev Immunol*. 2017;17:233-247.
31. Lee KM, Nam K, Oh S, et al. ECM1 regulates tumor metastasis and CSC-like property through stabilization of beta-catenin. *Oncogene*. 2015;34:6055-6065.

32. Lee KM, Nam K, Oh S, et al. Extracellular matrix protein 1 regulates cell proliferation and trastuzumab resistance through activation of epidermal growth factor signaling. *Breast Cancer Res*. 2014;16:479.
33. Long S, Wang J, Weng F, Xiang D, Sun G. Extracellular matrix protein 1 regulates colorectal cancer cell proliferative, migratory, invasive and epithelial-mesenchymal transition activities through the PI3K/AKT/GSK3beta/snail signaling Axis. *Front Oncol*. 2022;12:889159.
34. Chen C, Shan H. Keratin 6A gene silencing suppresses cell invasion and metastasis of nasopharyngeal carcinoma via the beta-catenin cascade. *Mol Med Rep*. 2019;19:3477-3484.
35. Kenny PA, Enver T, Ashworth A. Receptor and secreted targets of Wnt-1/beta-catenin signalling in mouse mammary epithelial cells. *BMC Cancer*. 2005;5:3.
36. Gong JH, Zheng YB, Zhang MR, et al. Dexamethasone enhances the antitumor efficacy of gemcitabine by glucocorticoid receptor signaling. *Cancer Biol Ther*. 2020;21:332-343.
37. Wang Y, Su J, Zhou P, et al. Glucocorticoids promote lung metastasis of pancreatic cancer cells through enhancing cell adhesion, migration and invasion. *Endocr J*. 2023;70:731-743.
38. Obradovic MMS, Hamelin B, Manevski N, et al. Glucocorticoids promote breast cancer metastasis. *Nature*. 2019;567:540-544.
39. Pang JM, Huang YC, Sun SP, et al. Effects of synthetic glucocorticoids on breast cancer progression. *Steroids*. 2020;164:108738.

SUPPORTING INFORMATION

Additional supporting information can be found online in the Supporting Information section at the end of this article.

How to cite this article: Shinomiya Y, Kouchi Y, Harada-Kagitani S, et al. ECM1 and KRT6A are involved in tumor progression and chemoresistance in the effect of dexamethasone on pancreatic cancer. *Cancer Sci*. 2024;115:1948-1963. doi:10.1111/cas.16175